Neurotoxicity Research (2022) 40:78–88
https://doi.org/10.1007/s12640-021-00456-5

ORIGINAL ARTICLE

VSIG4 Attenuates NLRP3 and Ameliorates Neuroinflammation via JAK2-STAT3-A20 Pathway after Intracerebral Hemorrhage in Mice

Na Ji[1] · Lirong Wu[2] · Hui Shi[3] · Qianlu Li[3] · Anyong Yu[4] · Zhao Yang[3]

Received: 9 October 2021 / Revised: 30 November 2021 / Accepted: 1 December 2021 / Published online: 11 January 2022

Abstract

Intracerebral hemorrhage (ICH) is a fatal cerebrovascular disease. Neuroinflammation plays an important pathological role in brain injury after ICH. NLRP3 contributes to the pathogenesis of ICH, but the underlying mechanisms regulating of NLRP3 remain elusive. V-set and immunoglobulin domain containing 4 (VSIG4), specifically expressed in resting tissue-resident macrophages, can deliver anti-inflammatory signals into various inflammatory diseases. However, the interaction between VSIG4 and NLRP3, as well as the underlying mechanisms after ICH have not been reported. C57BL/6 mice were subjected to the autologous blood injection ICH model. VSIG4 and NLRP3 levels of macrophages were detected following ICH. Ad-VSIG4 or controls were administered via intracerebroventricular (i.c.v) injection before ICH induction. STAT3 inhibitor (S31-201), JAK2 inhibitor (TG101348), or Ad-A20 RNAi was administered to investigate the role of JAK2-STAT3-A20 pathway in VSIG4-mediated neuroinflammation after ICH. Pro-inflammatory cytokine production, BBB disruption, brain water content, and neurological test were examined in ICH mice. VSIG4 levels were significantly decreased, and NLRP3 levels were significantly increased in the perihematomal brain tissues after ICH. Ad-VSIG4 attenuated NLRP3 levels and inhibited inflammation, as well as improved neurological function and reduced BBB disruption and brain water content. Furthermore, Ad-VSIG4 increased the protein levels of phosphorylated JAK2 and STAT3, and A20 levels at 24 h after ICH. STAT3 inhibitor, JAK2 inhibitor, and A20 RNAi abolished the beneficial effects of Ad-VSIG4 after ICH. In summary, these data suggested that VSIG4 attenuated NLRP3 and ameliorated neuroinflammation via JAK2-STAT3-A20 pathway after intracerebral hemorrhage in mice. VSIG4 might be an ideal therapeutic target for ICH patients.

Keywords VSIG4 · NLRP3 · Neuroinflammation · ICH

Introduction

Intracerebral hemorrhage (ICH) is a stroke subtype, with high mortality and morbidity due to its large fatality rate and poor functional outcome (Panos et al. 2020; Ponamgi et al. 2020; Yang et al. 2008; Zhang et al. 2017). The released blood cells and blood components such as thrombin, as well as erythrocyte rupture, result in mechanical damage and secondary damage [4–6]. Therefore, the therapeutic strategy targeting inflammation as well as the blood–brain barrier (BBB) and edema is a promising approach for ICH (Chen et al. 2015; Deng et al. 2020; Hou et al. 2020; Zhu et al. 2018).

Inflammasomes are multiprotein complexes that are involved in caspase-1 activation and interleukin-1β (IL-1β) maturation as well as pyroptosis (Zhang et al. 2018). Though numerous inflammasomes have been reported, the NLRP3 inflammasome is the most extensively studied.

Na Ji and Lirong Wu contributed equally to this study and are regarded as co-first authors.

✉ Anyong Yu
anyongyu@163.com

✉ Zhao Yang
yangzhao5140@sohu.com

[1] Department of Anesthesia, Second Affiliated Hospital, Zhejiang University School of Medicine, Hangzhou 310009, China

[2] Department of Neurology, Chongqing Hospital of Traditional Chinese Medicine, Chongqing 400021, China

[3] Department of Neurology, Yongchuan Hospital, Chongqing Medical University, Chongqing 402160, China

[4] Emergency Department of Emergency, Affiliated Hospital of Zunyi Medical University, Guizhou 563003, China

NLRP3 inflammasome is stimulated by a variety of factors, including infection, tissue damage, and metabolic dysregulation, and then activated through an integrated cellular signal (Wynosky-Dolfi et al. 2014). Recent evidence demonstrate that NLRP3 inflammasome plays a vital role in inflammation after intracerebral hemorrhage (Feng et al. 2015).

VSIG4, also known as CRIg or Z39Ig, is a newly identified member of the B7 super family (Tanaka et al. 2012). The expression of VSIG4 is restricted to tissue macrophages, including peritoneal macrophages and liver residential Kupffer cells (Shin et al. 2018). It negatively modulates the inflammation process by causing T-cell anergy and activates macrophage immunity when binding to the C3b/iC3b (Zhang et al. 2021). VSIG4 mediates transcriptional inhibition of NLRP3 and Il-1β in macrophages (Huang et al. 2019). Nevertheless, whether VSIG4 is capable of manipulating NLRP3 after ICH remains elusive.

In this experiment, C57BL/6 mice were subjected to the ICH model, and the regulation role of VSIG4 on NLRP3 and specific mechanism were analyzed.

Methods

Animals

All experimental protocols for this study were approved by the Animal Ethics Committee of Chongqing Medical University. The study complied with the National Institutes of Health Guide for the Care and Use of Laboratory Animals and the ARRIVE (Animal Research: Reporting In Vivo Experiments) guidelines. C57BL/6 mice (male, weight about 25 g) were purchased from and bred at the Animal Center of Chongqing Medical University. All mice were housed in a light- and temperature-controlled room with free access to food and water.

ICH mouse model induction

Mice were anesthetized with 10% chloral hydrate (350 mg/kg) and were placed in a stereotaxic frame (Alcott Biotech, Shanghai, China). Through a hole drilled in the skull, a 32-gauge needle was implanted into the striatum, 2.0 mm lateral to the midline, 1.0 mm anterior to the coronal suture, and at a depth of 4.0 mm from the surface of the brain. Each mouse was microinjected with 25 µl of autologous whole blood (right striatum) taken from the tail vein over 10 min using a microinfusion pump (ALC-IP600, Alcott Biotech). Then, the needle was pulled out without blood reflux after 5 min of dwelling, and the wound was sutured. Only the mouse observed to have a neurological deficit was regarded as a successful model. The mice in the sham operation group had the same operation, but no blood was injected.

Intracerebroventricular injection

The in vivo transfection was performed according to the method described as follows: the stereotaxic coordinates were 0.5 mm posterior and 1.0 mm lateral to bregma and 2.5–3.0 mm ventral to the surface of the skull. The Ad-VSIG4, Ad-NLRP3 siRNA, Ad-A20 RNAi or control (1×10^9 plaque-forming units (Pfu), Sangon Biotech, Shanghai, China) were added to 2 µl of a 10-mg/ml solution prepared in 0.9% NaCl. In the inhibitor treatment experiments, mice were received intracerebroventricular injection of 0.9% NaCl (2 µl) in the presence of the STAT3 inhibitor S3I-201 (50 mM, Sigma-Aldrich), or the JAK2 inhibitor TG101348 (50 µM, Sigma-Aldrich), respectively. The solution was mixed gently, left for 15 min and then injected intracerebroventricularly (i.c.v.) using a micro syringe (Hamilton, NV, USA) under the guidance of the stereotaxic instrument (RWD Life Science).

BBB permeability

To evaluate BBB permeability, Evans blue (Aladdin, China) was injected intraperitoneally (100 µl of 4% solution in saline). After 3 h of circulation, mice were transcardially perfused with cold phosphate-buffered saline (0.1 M, PBS, pH7.4) under deep anesthesia. Afterwards, the brain was removed and divided into left and right hemispheres and stored at − 80 °C immediately. The right part of the brain was homogenized in 1100 µl PBS, sonicated, and centrifuged (12,000 g, 4 °C, 30 min). The supernatant was collected and added an equal amount of trichloroacetic acid (TCA) to incubate overnight by 4 °C. After centrifugation (12,000 g, 4 °C, 30 min), Evans blue stain was measured by spectrophotometer (Thermo Fisher Scientific, USA) at 610 nm.

Immunofluorescence staining

The mice were deeply anesthetized and were transcardially perfused with 20 ml ice-cold PBS followed by 20 ml of 4% paraformaldehyde at 24 h post-ICH. The whole brain was collected and then fixed in 4% paraformaldehyde for another 24 h. Afterwards, the brain was fixed in 20% sucrose solution until the tissue sinks to the bottom followed by fixing in 30% sucrose solution for another 24 h. After being frozen at − 25 °C, the brain was cut into 10 µm-thick coronal sections using a cryostat (CM1860; Leica Microsystems, Germany). To conduct double immunohistochemistry staining, the brain sections were incubated with primary antibody of CD11b, VSIG4, or NLRP3 (1:100, Santa Cruz) overnight at 4 °C. After being incubated with the appropriate secondary

antibody (1:200, Bioss) at 37 °C for 1 h, the sections were visualized and photographed with a fluorescence microscope (UHGLGPS, OLYMPUS, Japan). Microphotographs were analyzed with cellSens Standard software. The numbers of positive cells were identified and counted in three different fields in the perihematoma area from five random coronal sections per brain, and data were expressed as cells/field.

Histochemical evaluation of macrophage accumulation

The mice were deeply anesthetized and were transcardially perfused with 20 ml ice-cold PBS followed by 20 ml of 4% paraformaldehyde at 24 h post-ICH. After the mice were perfused and fixed, the perihematomal region of cerebral tissues were collected, fixed in 4% paraformaldehyde for 24 h, dehydrated in 30% sucrose solution for 48 h, embedded, frozen, and cut into 25 μm sections using a Leica CM1900 cryostat. The perihematomal region was treated with 3% H_2O_2 in 0.01 M phosphate-buffered saline (PBS) and preincubated in 5% normal goat serum. The samples were then incubated in a primary antibody solution containing rat anti-CD11b antibody (Serotec, Fullerton, CA, USA, 1:200) overnight at 4 °C. After washing, the samples were incubated in a secondary IgG antibody (1:200) for 1 h at room temperature (RT). Finally, the sections were incubated in horseradish peroxidase (HRP)-Streptavidin (1:200) for 1 h at RT, and the color reaction was conventionally developed with diaminobenzidine (DAB) and H_2O_2. For each animal, six representative sections of each brain were selected. IPP6.0 image processing software (Media Cybernetics, MD, USA) was utilized to count the number of positive cells.

Western blotting

Briefly, the mice were perfused with 0.01 mol/l phosphate-buffered saline after ICH, and the cerebral tissues from the perihematomal region were isolated ($n=5$). The perihematomal tissues were lysed in 1 ml of radioimmunoprecipitation assay lysis buffer, and then the protein was extracted, electrophoresed, and transferred onto polyvinylidene fluoride membranes (Amersham Pharmacia). The polyvinylidene fluoride membranes were incubated with primary antibodies overnight, followed by incubation with peroxidase-conjugated secondary antibodies for 6 h. The same membranes were probed with an antibody for glyceraldehyde 3-phosphate dehydrogenase (GAPDH). Protein signals were detected with an enhanced chemiluminescence system. The signals were quantified by scanning densitometry and computer-assisted image analysis. Protein levels were expressed as the ratio of the values of the detected protein band to the GAPDH band.

Evaluation of neurological scores

The neurological scores were assessed by Neurological Severity Scores, according to the motor, sensory, reflex, and balance tests. Neurological function was assessed on a scale of 1–18; a score of 1 point is regarded as the inability to perform the test or for the lack of a tested reflex. The higher the score, the more severe the injury (normal score: 2–3; maximal deficit score: 18).

Measurement of brain edema

Brain hemisphere was quickly separated and weighted to assess the wet weight (wW) using an electronic analytic balance. After drying the brain hemisphere in an oven at 100 °C for 24 h, dry tissue weight (dW) was assessed. The percentage of water was calculated according to the following formula: Brain water content (%) = (wW-dW)/wW × 100%.

Statistics analysis

The data are expressed as the mean ± SD of at least 3 separate experiments performed in triplicate. The differences between groups were determined with the Student's *t* tests and a one-way analysis of variance (ANOVA) using SPSS 13.0 software. Differences were declared significant at $^*P<0.05$.

Results

VSIG4 and NLRP3 expressions in the perihematomal brain tissues after ICH

The expression of VSIG4 and NLRP3 proteins in perihematomal brain tissues after ICH was quantified using western blotting at the indicated time points (12, 24, and 72 h after ICH). The expression of VSIG4 started decreasing at 12 h and peaked at 24 h after ICH ($P<0.05$; Fig. 1A). The expression of NLRP3 started increasing at 12 h and peaked at 24 h after ICH ($P<0.05$; Fig. 1B). The representative images of double immunofluorescence staining of VSIG4 and NLRP3 expressions in $CD11b^+$ macrophage of the perihematomal brain tissues at 24 h after ICH are shown in Fig. 1C.

Upregulation of VSIG4 decreased the NLRP3 expression at 24 h after ICH

Mice were received intracerebroventricular injection of Ad-VSIG4 at 24 h before ICH. The expression of VSIG4 and NLRP3 proteins in perihematomal brain tissues after ICH was quantified using western blotting at 24 h after ICH. The expression of VSIG4 significantly increased after Ad-VSIG4

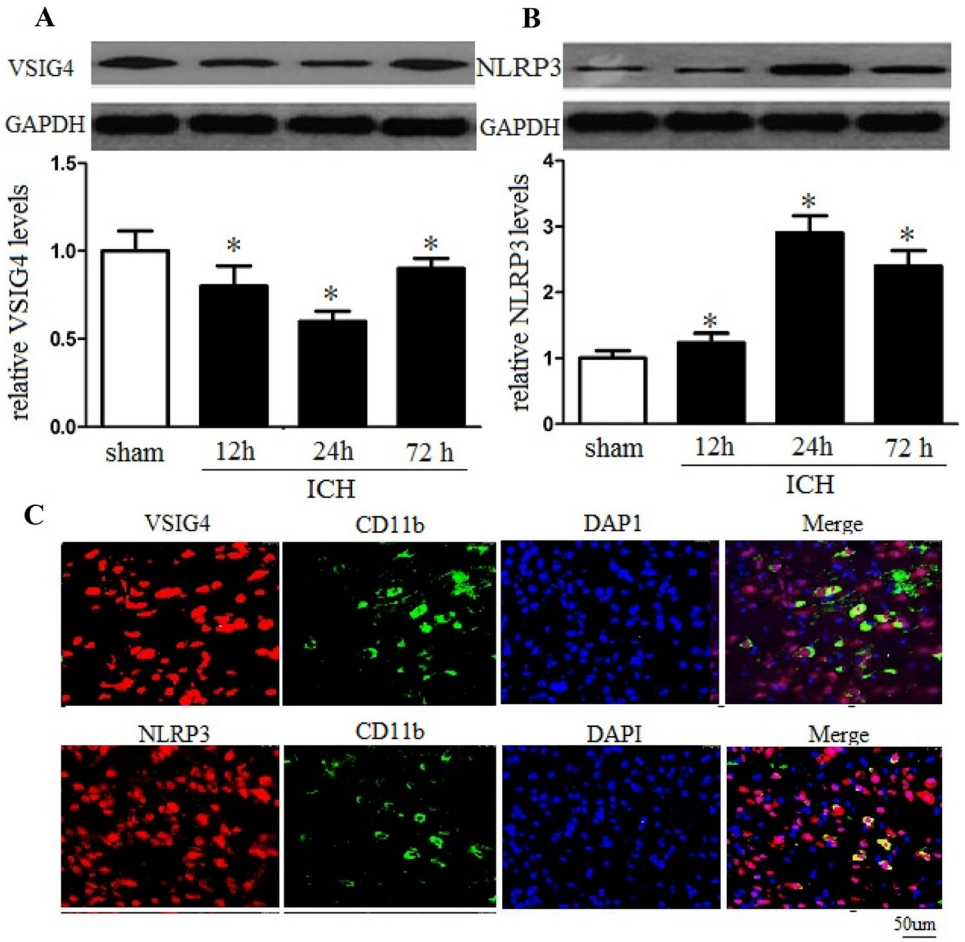

Fig. 1 VSIG4 and NLRP3 expressions in the perihematomal brain tissues after ICH. After 24 h after ICH, mice ($n=5$ per group) were deeply anesthetized in a transcardial manner. **A**, **B** The brains were removed and post fixed. The perihematomal region of cerebral tissue was collected, VSIG4 and NLRP3 expressions were analyzed with western blot analysis. **C** Representative images of double immunofluorescence staining of VSIG4 or NLRP3 colocalized with macrophage (CD11b) at 24 h after ICH. Scale bar = 50 μm. Experiments performed in triplicate showed consistent results. Data are presented as the mean ± standard error of mean (SEM) of three independent experiments. *$P<0.05$

injection compared with that of the control groups. However, NLRP3 significantly decreased after Ad-VSIG4 injection compared with that of the control groups ($P<0.05$; Fig. 2A, B). The representative images of double immunofluorescence staining of VSIG4 or NLRP3 expression in the macrophage of the perihematomal brain tissues at 24 h after ICH are shown in Fig. 2C. $CD11b^+$ macrophage numbers were not decreased after Ad-VSIG4 treatment, but NLRP3 + $CD11b^+$ macrophage numbers decreased after Ad-VSIG4 treatment compared with that of the control groups ($P<0.05$; Fig. 2D).

Upregulation of VSIG4 improved neurological deficits and reduced brain edema and BBB permeability after ICH

To further evaluate the role of VSIG4 on the ICH-induced neurological impairment, we injected Ad-VSIG4 at 24 h before ICH. The neurological deficits and brain edema were worse at 24 h post-ICH compared with the sham group. However, administration of Ad-VSIG4 significantly improved the neurological deficits and reduced brain edema ($P<0.05$; Fig. 3A, B). BBB permeability was assessed by EB extravasation assay. EB extravasation in the ICH group was significantly increased at 24 h after ICH; however, Ad-VSIG4 significantly decreased EB dye leakage compared with that of the control group (Fig. 3C).

Knockdown of NLRP3 aggravated neurological deficits, brain edema, and BBB disruption after ICH

To further investigate the protective role of VSIG4, NLRP3 siRNA was administered by i.c.v injection to knock down the expression of endogenous NLRP3. Western blot showed that NLRP3 expression was inhibited by NLRP3 siRNA at 24 h after injection (Fig. 4A). The knockdown of NLRP3 abolished the protective effect of VSIG4 on neurological functions, brain edema, and BBB integrity at 24 h after ICH (Fig. 4B–D).

Upregulation of VSIG4 inhibited macrophage accumulation and downstream molecule expression in ICH

To determine whether VSIG4 could attenuate ICH-induced neuroinflammation in mice, macrophage accumulation and

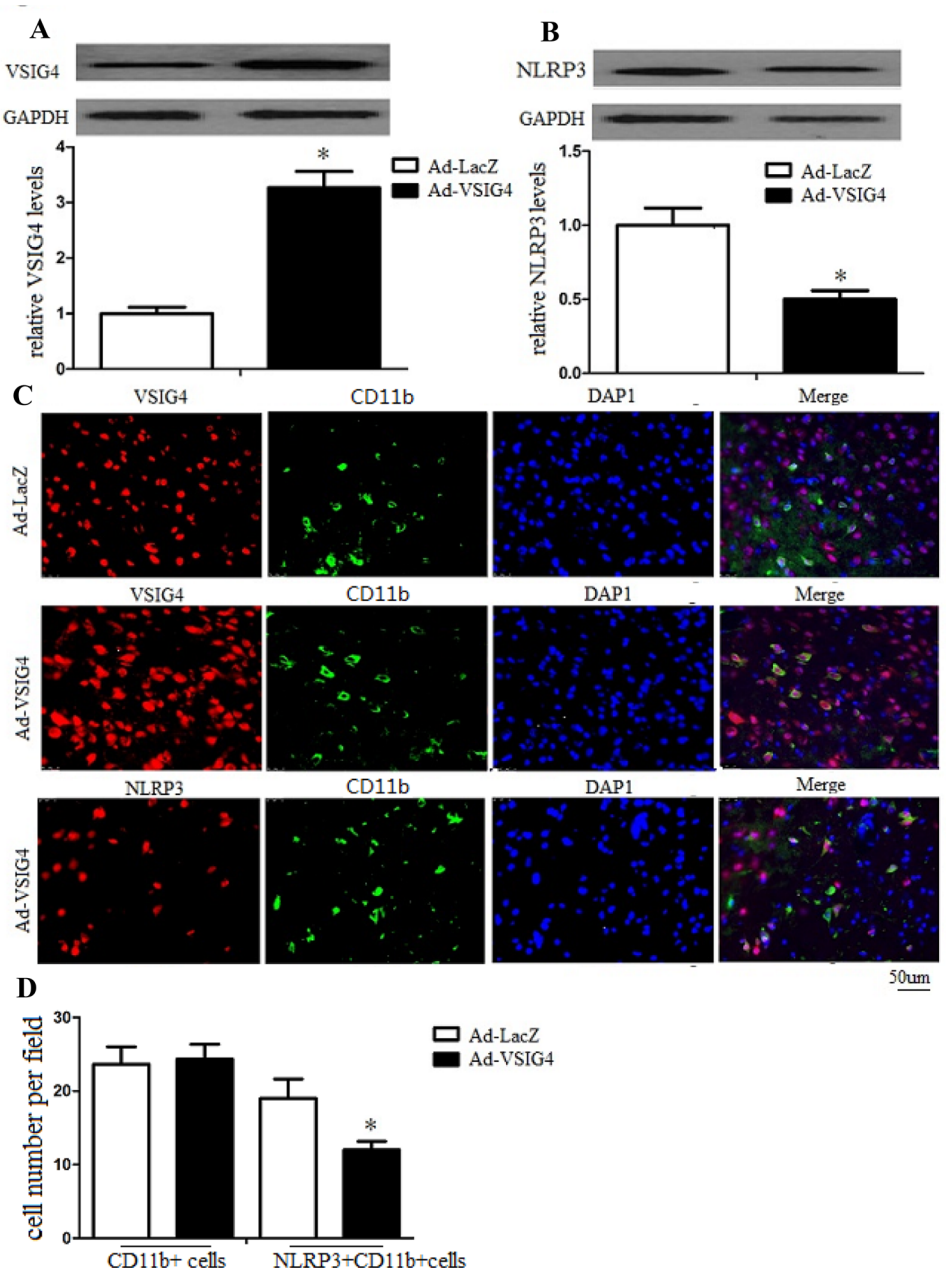

Fig. 2 Upregulation of VSIG4 decreased the NLRP3 expression at 24 h after ICH. Mice were received intracerebroventricular injection of Ad-VSIG4 at 24 h before ICH. After 24 h after ICH, mice ($n=5$ per group) were deeply anesthetized in a transcardial manner. **A**, **B** The brains were removed and post fixed. The perihematomal region of cerebral tissue was collected, VSIG4 and NLRP3 expressions were analyzed with western blot analysis. **C** Representative images of double immunofluorescence staining of VSIG4 or NLRP3 colocalized macrophage (CD11b) at 24 h after ICH. Scale bar = 50 μm. **D** $CD11b^+$ or NLRP3 + $CD11b^+$ macrophage numbers after Ad-VSIG4 or Ad-LacZ treatment. Experiments performed in triplicate showed consistent results. Data are presented as the mean ± standard error of mean (SEM) of three independent experiments. $^*P<0.05$

downstream molecules in the hippocampus were examined 24 h after ICH. Macrophage accumulation in the perihematomal brain tissues significantly increased compared with control mice after ICH. However, administration of Ad-VSIG4 could attenuate macrophage accumulation (Fig. 5A). ZO-1, occludin, and Lama5 in the perihematomal brain tissues significantly decreased, but TNF-α, IL-1β, and IL-6 protein levels in the perihematomal brain tissues significantly increased compared with those of the control mice 24 h after ICH. However, administration of Ad-VSIG4 could enhance ZO-1, occludin, and Lama5 and attenuate TNF-α, IL-1β, and IL-6 protein levels (Fig. 5B–H). These results suggest that upregulation of VSIG4 could inhibit ICH-induced neuroinflammation.

Upregulation of VSIG4 attenuated NLRP3 and ameliorated neuroinflammation by activating JAK2-STAT3-A20 pathway

We further investigated the underlying signaling pathways of VSIG4 inhibiting NLRP3. A20, a protein capable of downmodulating LPS, induced NLRP3 transcription through inhibiting NF-kβ activation. Treatment with Ad-VSIG4 increased the expression of JAK2, STAT3, and A20 in the perihematoma

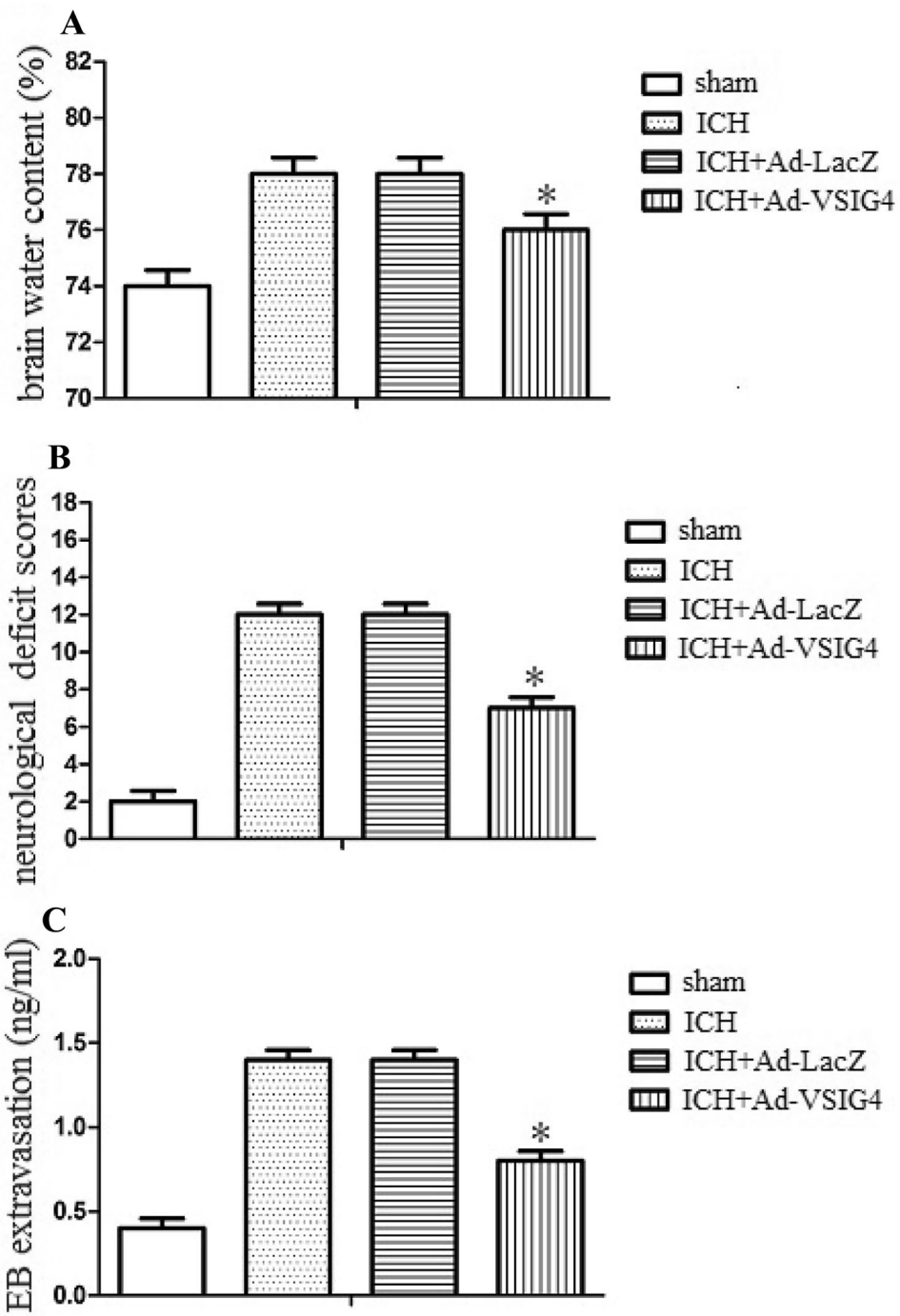

Fig. 3 Upregulation of VSIG4 improved neurological deficits and reduced brain edema and BBB permeability after ICH. Mice were received intracerebroventricular injection of Ad-VSIG4 at 24 h before ICH. After 24 h after ICH, mice ($n=5$ per group) were deeply anesthetized in a transcardial manner. **A** The brains were removed and post fixed. The perihematomal region of cerebral tissue was collected, VSIG4 expression was analyzed with western blot analysis. **B** The BBB disruption of mice was analyzed. **C** The cerebral water content of mice was also analyzed. **D** The neurological deficit tests were performed by behavioral measurement, including composite of motor, sensory, reflex, and balance tests. Experiments performed in triplicate showed consistent results. Data are presented as the mean ± standard error of mean (SEM) of three independent experiments. $^*P<0.05$

tissue at 24 h post-ICH compared with the control group (Fig. 6A). However, STAT3 inhibitor (S31-201), JAK2 inhibitor (TG101348), and Ad-A20 siRNA enhanced NLRP3 levels in the perihematoma tissue at 24 h post-ICH compared with the control group (Fig. 6B). In addition, STAT3 inhibitor (S31-201), JAK2 inhibitor (TG101348) inhibitor (TG10ion1348), and Ad-A20 siRNA exacerbated neurological impairments and increased brain water content at 24 h after ICH (Fig. 6C, D). Furthermore, STT3 inhibitor (S31-201), JAK2 inhibitor (TG101348) inhibitor (TG10ion1348), and Ad-A20 siRNA increased the expression of TNF-α, IL-1β, and IL-6 protein levels in the perihematomal brain tissues (Fig. 6E).

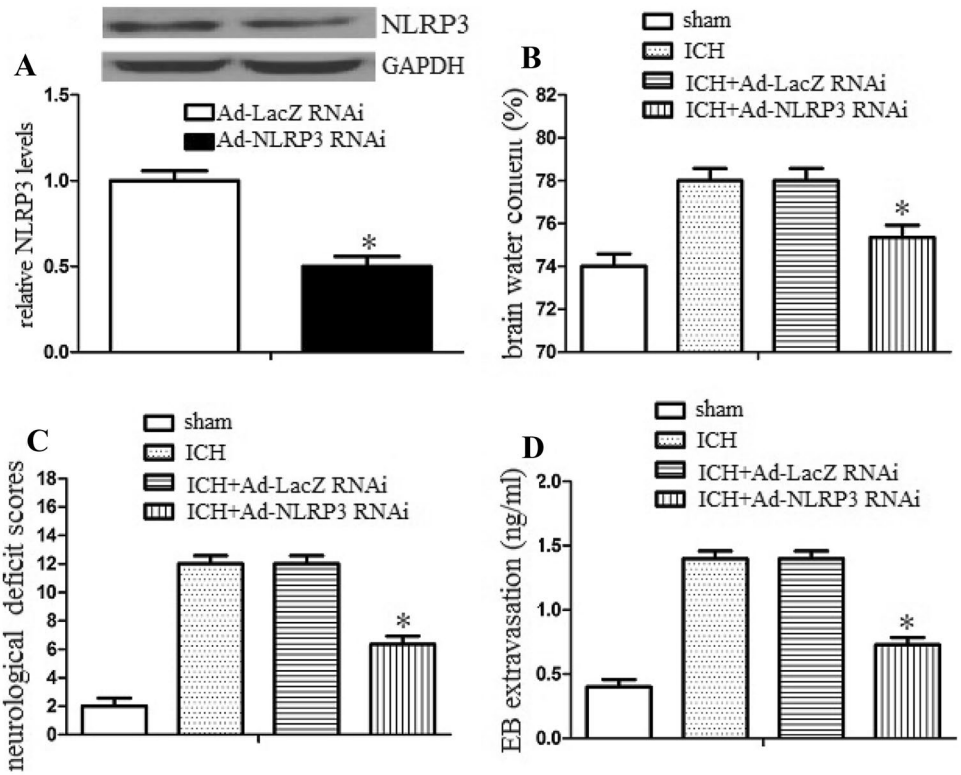

Fig. 4 Knockdown of NLRP3 aggravated neurological deficits, brain edema, and BBB disruption after ICH. Mice were received intracerebroventricular injection of Ad-NLRP3 siRNA at 24 h before ICH. After 24 h after ICH, mice ($n=5$ per group) were deeply anesthetized in a transcardial manner. **A** The brains were removed and post fixed. The perihematomal region of cerebral tissue was collected, NLRP3 expression was analyzed with western blot analysis. **B** The BBB disruption of mice was analyzed. **C** The cerebral water content of mice was also analyzed. **D** The neurological deficit tests were performed by behavioral measurement, including composite of motor, sensory, reflex, and balance tests. Experiments performed in triplicate showed consistent results. Data are presented as the mean ± standard error of mean (SEM) of three independent experiments. *$P<0.05$

Discussion

In this experiment, we presented the following evidences: (1) VSIG4 was significantly decreased, and NLRP3 was significantly increased in the perihematoma tissue after ICH; (2) upregulation of VSIG4 decreased the NLRP3 expression following ICH; (3) upregulation of VSIG4 improved neurological deficits and reduced brain edema and BBB permeability after ICH; (4) knockdown of NLRP3 aggravated neurological deficits, brain edema, and BBB disruption after ICH; (5) upregulation of VSIG4 inhibited macrophage accumulation and downstream molecule expression in ICH; (6) upregulation of VSIG4 attenuated NLRP3 and ameliorated neuroinflammation by activating the JAK2-STAT3-A20 pathway.

Numerous data indicated that inflammation and BBB disruption are important points to induce secondary brain damage following ICH (Cheng et al. 2016; Li et al. 2020; Wang et al. 2019). Following ICH, blood components rapidly enter the cerebral parenchyma, leading to an inflammatory reaction. Furthermore, intensive inflammatory cascades enhance BBB disruption, resulting in blood component infiltration into the brain, and subsequent exacerbation of brain damage after ICH (Cai et al. 2015; Wu et al. 2020; Xi et al. 2002).

The NLRP3 inflammasome amplified the inflammatory response by releasing IL-1β and promoting neutrophil infiltration following ICH (Chen et al. 2014; Gicquel et al. 2015; Ma et al. 2014). The activation of the NLRP3 inflammasome is tightly regulated at the transcriptional and post-translational levels to inhibit excessive inflammation in the host (Karasawa et al. 2018; Surabhi et al. 2020; Zheng et al. 2020). Therefore, identification and exploring of unknown factors regulating the NLRP3 inflammasome might represent a promising strategy for ICH. VSIG4 is a member of the B7 family-related protein which is well-known for its inhibition of T-cell activation and works as a co-inhibitory ligand that inhibits T-cell activation and cytokine production through cell cycle arrest at the G0/G1 phase and induces T-cell anergy (Deng et al. 2019; Wang et al. 2015; Zhai et al. 2018). The relationship between VSIG4 and NLRP3 after ICH has not been studied. In our experiment, we firstly detected VSIG4 and NLRP3 levels in the macrophage after

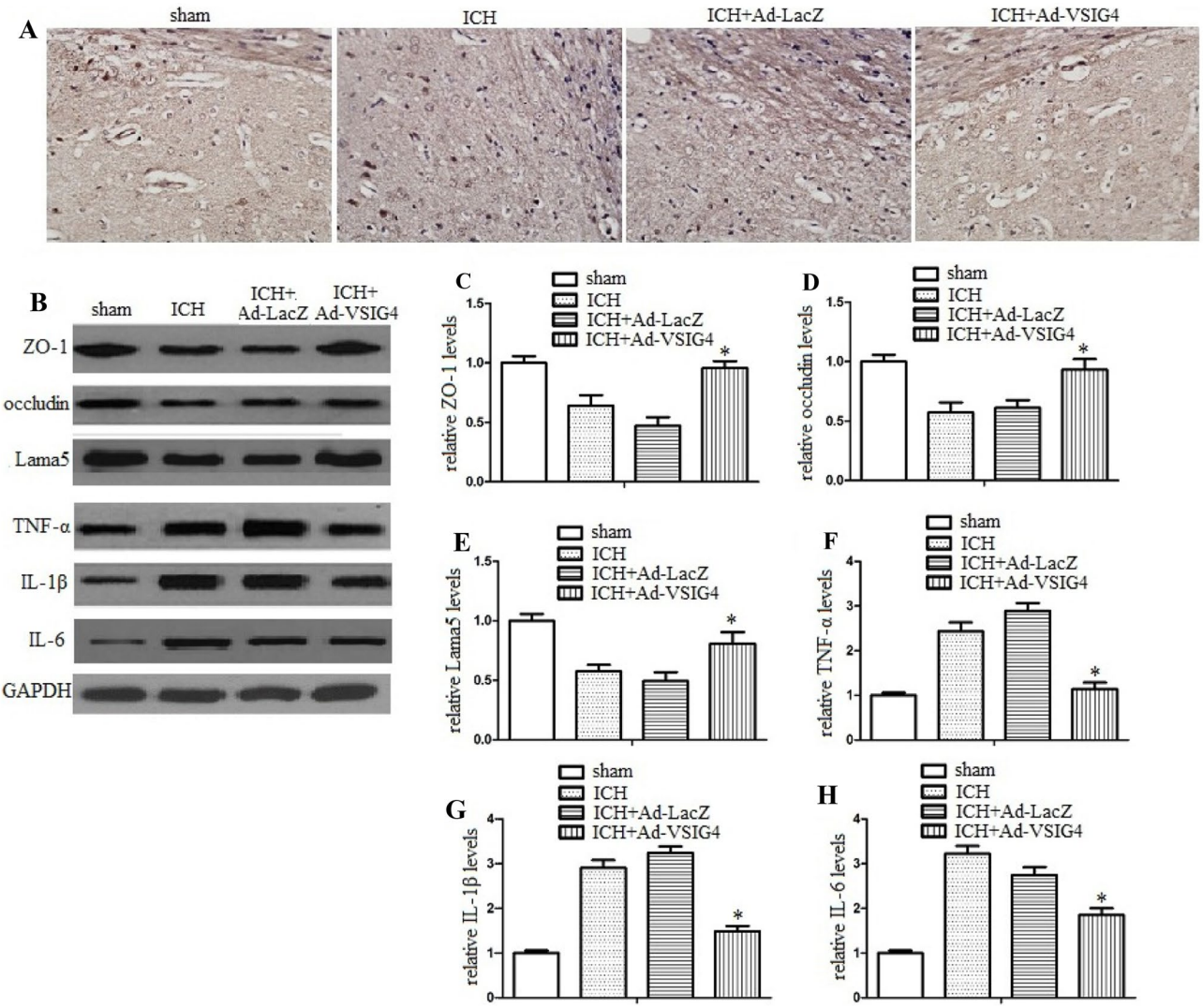

Fig. 5 Upregulation of VSIG4 inhibited macrophage accumulation and downstream molecule expression in ICH. Mice were received intracerebroventricular injection of Ad-VSIG4 at 24 h before ICH. After 24 h after ICH, mice ($n=5$ per group) were deeply anesthetized in a transcardial manner. The brains were removed and post fixed. **A** Representative images of histochemical evaluation of macrophage (CD11b) at 24 h after ICH. Scale bar = 50 μm. **B**–**H** ZO-1, occludin, Lama5, TNF-α, IL-1β, and IL-6 protein levels in the perihematomal brain tissues were analyzed with western blot analysis. Experiments performed in triplicate showed consistent results. Data are presented as the mean ± standard error of mean (SEM) of three independent experiments. $^*P<0.05$

ICH, and found that upregulation of VSIG4 decreased the NLRP3 expression at 24 h after ICH. Secondly, we evaluated the role of VSIG4 on the ICH and found that VSIG4 improved neurological deficits and reduced brain edema and BBB permeability after ICH.

A20 is an endogenous anti-inflammatory factor that can attenuate the destructive proinflammatory factor production such as IL-1β and TNF-α by inhibiting NF-kβ activation (Yao et al. 2018). A20 also interacts with IL-10 and TGF-β and inhibits inflammation in diabetes and arthritis (Liuwantara et al. 2006; Vereecke et al. 2009). A20 has been shown to attenuate NLRP3 inflammasome activity, and macrophage A20-deficient mice show exacerbated CNS inflammation due to hyperactivation of the NLRP3 inflammasome that leads to increased IL-1β secretion and CNS inflammation (Gupta et al. 2017; Mohebiany et al. 2020). Our data demonstrated that treatment with Ad-VSIG4 increased the expression of JAK2, STAT3, and A20 in the perihematoma tissue at 24 h post-ICH compared with that of the control group. However, STAT3 inhibitor (S31-201), JAK2 inhibitor (TG101348) inhibitor (TG101348), and Ad-A20 siRNA enhanced NLRP3 levels in the perihematoma tissue, proinflammatory cytokine production and BBB disruption, exacerbated neurological impairments and increased brain water content at 24 h after ICH.

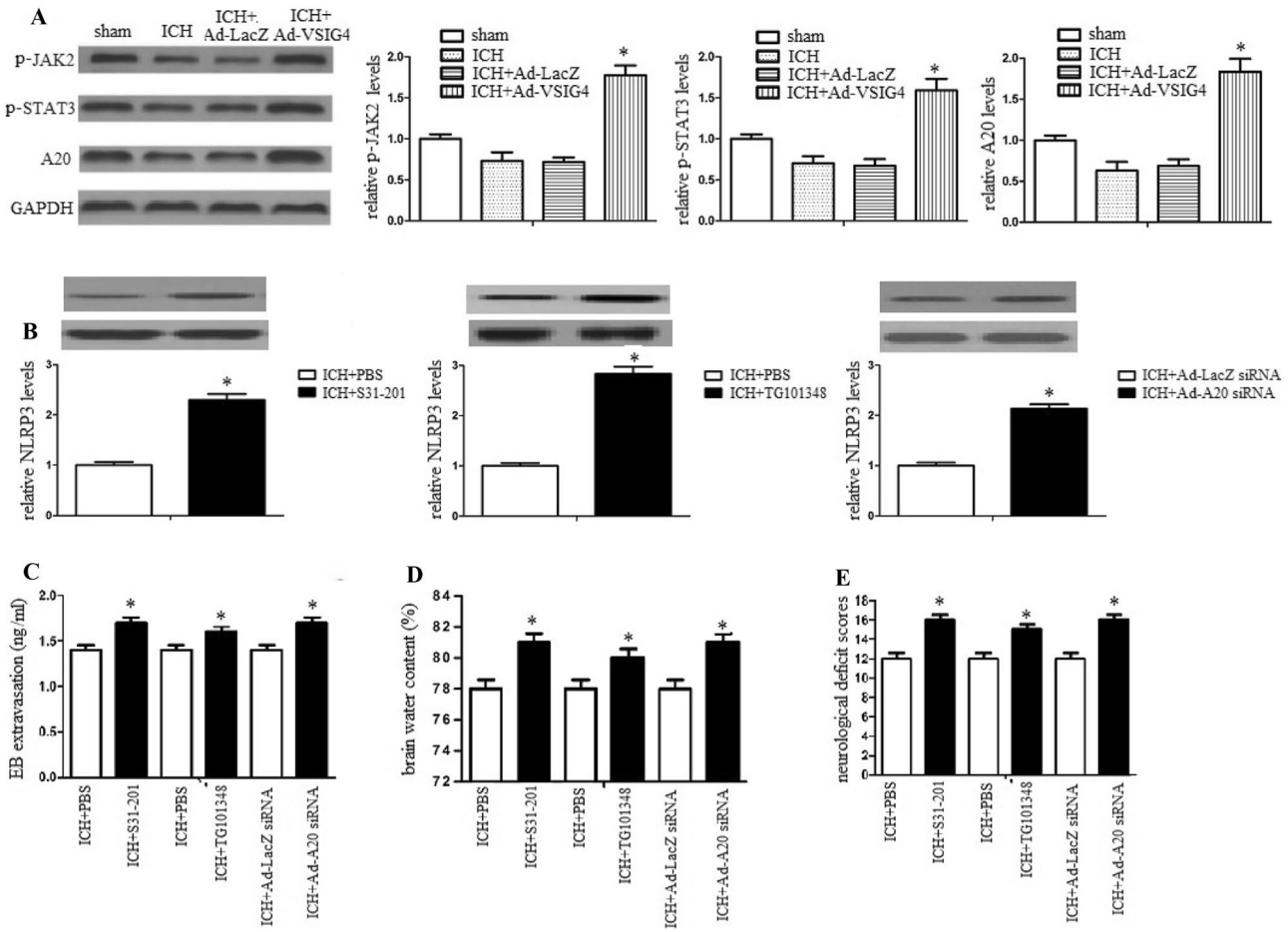

Fig. 6 Upregulation of VSIG4 attenuated NLRP3 and ameliorated brain injury by activating JAK2-STAT3-A20 pathway. Mice were received intracerebroventricular injection of Ad-VSIG4 at 24 h before ICH. After 24 h after ICH, mice ($n=5$ per group) were deeply anesthetized in a transcardial manner. The brains were removed and post fixed. **A** p-JAK2, p-STAT3, and A20 in the perihematoma tissue were analyzed with western blot analysis. **B** STAT3 inhibitor (S31-201), JAK2 inhibitor (TG101348), and Ad-A20 siRNA were pretreated at 24 h before ICH, NLRP3 in the perihematoma tissue were analyzed with western blot analysis. **C** The BBB disruption of mice was analyzed. **D** The cerebral water content of mice was also analyzed. **E** The neurological deficit tests were performed by behavioral measurement, including composite of motor, sensory, reflex, and balance tests. Experiments performed in triplicate showed consistent results. Data are presented as the mean ± standard error of mean (SEM) of three independent experiments. *$P<0.05$

Conclusion

VSIG4 could attenuate neuroinflammation and BBB disruption and improve neurological impairments after ICH in mice. The neuroprotective role of VSIG4 activated the cascade JAK2-STAT3-A20 signaling pathway, leading to NLRP3 inhibition. Therefore, VSIG4-NLRP3 might serve as a potential therapeutic agent against neuroinflammation for ICH patients.

Author contributions NJ designed the research. LRW performed the research. AYY analyzed the data. ZY wrote the manuscript. All authors read and approved the final manuscript.

Funding This work was supported by the National Natural Science Foundation of China (82060245) and ycstc-jckx20027.

Availability of data and materials The data used in the present study are available from the corresponding author on reasonable request.

Declarations

Ethics approval and consent to participate All experimental protocols for this study were approved by the Animal Ethics Committee of Chongqing Medical University in accordance with the National Institutes of Health guidelines for the care and use of experimental animals.

Consent for publication Not applicable.

Competing interests The authors declare no competing interests.

References

Cai P, Luo H, Xu H, Zhu X, Xu W, Dai Y, Xiao J, Cao Y, Zhao Y, Zhao BQ et al (2015) Recombinant ADAMTS 13 attenuates brain injury after intracerebral hemorrhage. Stroke 46:2647–2653

Chen Q, Jin Y, Zhang K, Li H, Chen W, Meng G, Fang X (2014) Alarmin HNP-1 promotes pyroptosis and IL-1β release through different roles of NLRP3 inflammasome via P2X7 in LPS-primed macrophages. Innate Immun 20:290–300

Chen S, Yang Q, Chen G, Zhang JH (2015) An update on inflammation in the acute phase of intracerebral hemorrhage. Transl Stroke Res 6:4–8

Cheng S, Gao W, Xu X, Fan H, Wu Y, Li F, Zhang J, Zhu X, Zhang Y (2016) Methylprednisolone sodium succinate reduces BBB disruption and inflammation in a model mouse of intracranial haemorrhage. Brain Res Bull 127:226–233

Deng G, Chen W, Wang P, Zhan T, Zheng W, Gu Z, Wang X, Ji X, Sun Y (2019) Inhibition of NLRP3 inflammasome-mediated pyroptosis in macrophage by cycloastragenol contributes to amelioration of imiquimod-induced psoriasis-like skin inflammation in mice. Int Immunopharmacol 74:105682

Deng S, Sherchan P, Jin P, Huang L, Travis Z, Zhang JH, Gong Y, Tang J (2020) Recombinant CCL17 enhances hematoma resolution and activation of CCR4/ERK/Nrf2/CD163 signaling pathway after intracerebral hemorrhage in mice. Neurotherapeutics: the journal of the American Society for Experimental NeuroTherapeutics 17:1940–1953

Feng L, Chen Y, Ding R, Fu Z, Yang S, Deng X, Zeng J (2015) P2X7R blockade prevents NLRP3 inflammasome activation and brain injury in a rat model of intracerebral hemorrhage: involvement of peroxynitrite. J Neuroinflammation 12:190

Gicquel T, Robert S, Loyer P, Victoni T, Bodin A, Ribault C, Gleonnec F, Couillin I, Boichot E, Lagente V (2015) IL-1β production is dependent on the activation of purinergic receptors and NLRP3 pathway in human macrophages. FASEB Journal : Official Publication of the Federation of American Societies for Experimental Biology 29:4162–4173

Gupta AK, Ghosh K, Palit S, Barua J, Das PK, Ukil A (2017) Leishmania donovani inhibits inflammasome-dependent macrophage activation by exploiting the negative regulatory proteins A20 and UCP2. FASEB Journal : Official Publication of the Federation of American Societies for Experimental Biology 31:5087–5101

Hou Y, Hu Z, Gong X, Yang B (2020) HSPB8 overexpression prevents disruption of blood-brain barrier after intracerebral hemorrhage in rats through Akt/GSK3β/β-catenin signaling pathway. Aging 12:17568–17581

Huang X, Feng Z, Jiang Y, Li J, Xiang Q, Guo S, Yang C, Fei L, Guo G, Zheng L et al (2019) VSIG4 mediates transcriptional inhibition of Nlrp3 and Il-1β in macrophages. Sci Adv 5:eaau7426

Karasawa T, Kawashima A, Usui-Kawanishi F, Watanabe S, Kimura H, Kamata R, Shirasuna K, Koyama Y, Sato-Tomita A, Matsuzaka T et al (2018) Saturated fatty acids undergo intracellular crystallization and activate the NLRP3 inflammasome in macrophages. Arterioscler Thromb Vasc Biol 38:744–756

Li Z, Li M, Shi SX, Yao N, Cheng X, Guo A, Zhu Z, Zhang X, Liu Q (2020) Brain transforms natural killer cells that exacerbate brain edema after intracerebral hemorrhage. J Exp Med 217

Liuwantara D, Elliot M, Smith MW, Yam AO, Walters SN, Marino E, McShea A, Grey ST (2006) Nuclear factor-kappaB regulates beta-cell death: a critical role for A20 in beta-cell protection. Diabetes 55:2491–2501

Ma Q, Chen S, Hu Q, Feng H, Zhang JH, Tang J (2014) NLRP3 inflammasome contributes to inflammation after intracerebral hemorrhage. Ann Neurol 75:209–219

Mohebiany AN, Ramphal NS, Karram K, Di Liberto G, Novkovic T, Klein M, Marini F, Kreutzfeldt M, Härtner F, Lacher SM et al (2020) Microglial A20 protects the brain from CD8 T-cell-mediated immunopathology. Cell Rep 30:1585-1597.e6

Panos NG, Cook AM, John S, Jones GM (2020) Factor Xa inhibitor-related intracranial hemorrhage: results from a multicenter, observational cohort receiving prothrombin complex concentrates. Circulation 141:1681–1689

Ponamgi SP, Ward R, DeSimone CV, English S, Hodge DO, Slusser JP, Graff-Radford J, Rabinstein AA, Asirvatham SJ, Holmes Jr D (2020) High mortality rates among patients with non-traumatic intracerebral hemorrhage and atrial fibrillation on antithrombotic therapy are independent of the presence of cerebral amyloid angiopathy: insights from a population-based study. J Am Heart Assoc 9:e016893

Shin W, Jeon Y, Choi I, Kim YJ (2018) V-set and Ig domain-containing 4 (VSIG4)-expressing hepatic F4/80(+) cells regulate oral antigen-specific responses in mouse. Eur J Immunol 48:632–643

Surabhi S, Cuypers F, Hammerschmidt S, Siemens N (2020) The role of NLRP3 inflammasome in pneumococcal infections. Front Immunol 11:614801

Tanaka M, Nagai T, Usami M, Hasui K, Takao S, Matsuyama T (2012) Phenotypic and functional profiles of CRIg (Z39Ig)-expressing macrophages in the large intestine. Innate Immun 18:258–267

Vereecke L, Beyaert R, van Loo G (2009) The ubiquitin-editing enzyme A20 (TNFAIP3) is a central regulator of immunopathology. Trends Immunol 30:383–391

Wang G, Li Z, Li S, Ren J, Suresh V, Xu D, Zang W, Liu X, Li W, Wang H et al (2019) Minocycline preserves the integrity and permeability of BBB by altering the activity of DKK1-Wnt signaling in ICH model. Neuroscience 415:135–146

Wang X, Wang S, Hu C, Chen W, Shen Y, Wu X, Sun Y, Xu Q (2015) A new pharmacological effect of levornidazole: inhibition of NLRP3 inflammasome activation. Biochem Pharmacol 97:178–188

Wu D, Lai N, Deng R, Liang T, Pan P, Yuan G, Li X, Li H, Shen H, Wang Z et al (2020) Activated WNK3 induced by intracerebral hemorrhage deteriorates brain injury maybe via WNK3/SPAK/NKCC1 pathway. Exp Neurol 332:113386

Wynosky-Dolfi MA, Snyder AG, Philip NH, Doonan PJ, Poffenberger MC, Avizonis D, Zwack EE, Riblett AM, Hu B, Strowig T et al (2014) Oxidative metabolism enables Salmonella evasion of the NLRP3 inflammasome. J Exp Med 211:653–668

Xi G, Keep RF, Hoff JT (2002) Pathophysiology of brain edema formation. Neurosurg Clin N Am 13:371–383

Yang Z, Wang L, Wang H, Shang X, Niu W, Li J, Wu Y (2008) A novel mimovirus vaccine containing survivin epitope with adjuvant IL-15 induces long-lasting cellular immunity and high antitumor efficiency. Mol Immunol 45:1674–1681

Yao D, Xu L, Xu O, Li R, Chen M, Shen H, Zhu H, Zhang F, Yao D, Chen YF et al (2018) O-linked β-N-acetylglucosamine modification of A20 enhances the inhibition of NF-κB (nuclear factor-κB) ativation and elicits vascular protection after acute endoluminal arterial injury. Arterioscler Thromb Vasc Biol 38:1309–1320

Zhai Y, Lin P, Feng Z, Lu H, Han Q, Chen J, Zhang Y, He Q, Nan G, Luo X et al (2018) TNFAIP3-DEPTOR complex regulates inflammasome secretion through autophagy in ankylosing spondylitis monocytes. Autophagy 14:1629–1643

Zhang D, Shen X, Pang K, Yang Z, Yu A (2021) VSIG4 alleviates intracerebral hemorrhage induced brain injury by suppressing TLR4-regulated inflammatory response. Brain Res Bull 176:67–75

Zhang L, Liu Y, Wang B, Xu G, Yang Z, Tang M, Ma A, Jing T, Xu X, Zhang X et al (2018) POH1 deubiquitinates pro-interleukin-1β and restricts inflammasome activity. Nat Commun 9:4225

Zhang Z, Zhang Z, Lu H, Yang Q, Wu H, Wang J (2017) Microglial polarization and inflammatory mediators after intracerebral hemorrhage. Mol Neurobiol 54:1874–1886

Zheng S, Ma M, Li Z, Hao Y, Li H, Fu P, Jin S (2020) Posttreatment of maresin1 inhibits NLRP3 inflammasome activation via promotion of NLRP3 ubiquitination. FASEB Journal : Official Publication of the Federation of American Societies for Experimental Biology 34:11944–11956

Zhu Q, Enkhjargal B, Huang L, Zhang T, Sun C, Xie Z, Wu P, Mo J, Tang J, Xie Z et al (2018) Aggf1 attenuates neuroinflammation and BBB disruption via PI3K/Akt/NF-κB pathway after subarachnoid hemorrhage in rats. J Neuroinflammation 15:178